Ibn Al-Haitham Journal for Pure and Applied Sciences
Journal homepage: jih.uobaghdad.edu.iq
PISSN: 1609-4042, EISSN: 2521-3407
IHJPAS. 2026; 39(1)

Carbon Black in Electromagnetic Interference Shielding Effectiveness of Lightweight Polypyrrole in (C-Band and X-Band) Frequency Range

Ali N. Obead[1] and Nadia A. Ali [2*]
[1,2]Department of Physics, College of Science, University of Baghdad, Baghdad, Iraq.
*Corresponding Author.

Received: 21/May/2025
Accepted:31/August/2025
Published:20/January/2026
doi.org/10.30526/39.1.4201

Abstract

EMI (Electromagnetic Interference) shielding apeara lot of attention of that electronic devices are being used more widely and reports design progress for shielding..The EMI of PPy/Carbon black synthesized different weight (0,1,3,5 wt.%) of C.B using chemical oxidation method at (3-7)°C and charactrized with X-ray diffraction, Fourier transformation, Field Emission scanning electron microscopy, Electrical conductivity, high Electromagnetic Shielding Effectiveness (SE) in a frequency range of 5.85- 8.2GHz (C-band), 8.20-12.40 GHz (x-band),and thermal analyzed using differential thermal analysis (TGA-DSC). FTIR reveal the required functional groups that should be present in all nanocomposites. The dispersion and formed a network of conductive phases that composites had a rough surface and a porous structure of the carbon black particles, according to FESEM results. The PPy/ C.B with the A.C conductivity (3.04*10-3) S/cm exhibited shielding efficiency SE in (C-band) at (-33dB) is highly dependent on carbon black and thickness 1.5 mm , with the maximum SE attenuation recorded at 5wt% of carbon black being (-36dB) at 12 GHz. Also in (X-band) that SE attenuation recorded being at 8GHz . All PPy/C.B nanocomposites exhibit decreasing dielectric properties (ε′, ε′′, tan δ) with increasing frequency .These nanocomposites demonstrate effective EMI shielding and can be used in various applications such as molecular electronics and microwave absorption materials. Test of TGA-DSC show that exothermic reactions with the dominating weight% take place in (25-800) °C, the glass transition temperatures (Tg) at low and high contents of PPy/C.B nanocomposites between (110-160 °C). The obtained values of Tg showed complete miscibility of most composites. Thermo-gravimetric analysis showed that the Carbon black in polypyrrole nanocomposites formula has highest thermal stability with improved degradation temperature at 660-669 0C at 5% weight loss.

Keywords: Electromagnetic interference (EM) shielding, (8-12GHz, 5.2- 8GHz), A.C electrical conductivity, Dielectric constant properties, TGA-DSC.

1. Introduction

Nowadays, trouble from electromagnetic interference (EMI) is becoming more serious, thanks to the progress in digital devices like high-speed processors, Doppler radar, telecommunication, microwave darkrooms used for civil and military purposes, and weather forecasting systems[1]. The growing emission of radio waves results in these devices not functioning properly, and it has a damaging effect on both the environment and people[2]. Electronic items, such as telephones, radars, electrodes, and transmitters, are now used more frequently in areas, homes, and medicine. With this growth in technology, electromagnetic interference (EMI) is more likely, which refers

to signals that can negatively affect devices and living beings[3]. Eliminating and alleviating these adverse effects is possible by developing novel and high-performance EM shielding materials, which have drawn considerable attention in the relevant fields. Compared with traditional metal-based EM shielding materials, polymer-based EM shielding materials have essential performance parameters such as good processability, low cost, lightweight, flexibility in design, corrosion resistance, and a wide effective absorption bandwidth, which are often required in fields such as aerospace and aviation[4]. For that reason, researchers have created shielding materials that work to reduce and dissipate the presence of radiation. EMI-SE, which is measured in decibels (dB), describes the capacity of a material to resist electromagnetic fields [5].

Among the conductive polymer materials, (ICPs) and (ECSPs) that being watched closely for their ability to shield against EMI by absorbing EM waves and having them removed by the conductive particles used, something that matters greatly in various applications[6]. In addition, ECPCs composites it easy to fabricate and little corrosion, and the cost that containing intrinsically conducting polymers, carbonaceous fillers, such as CB, CNT, Gr, CNTF have been widely used in EMI shielding materials[7].

A number of studies have appeared on conducting polymers and their associated materials as functional nanomaterials for electromagnetic properties. Due to their low chemical potential, outstanding qualities in electrochemistry, high electrical conductivity, straightforward fabrication and good stability, different ICP polypyrrole-based nanomaterials are attracting significant attention Mondal[8]. In addition, research has moved forward on PPy-based nanomaterials for protecting from electromagnetic interference. It can exhibit conductivity within a wide range (from 10^{-3} Scm^{-1} to 100 Scm^{-1}) that is controlled by the monomer's structure[9]. Polypyrrole (PPy) is considered a promising material because it can dissipate microwaves in several ways, maintains its properties even outdoors, has tunable loss factors, and is straightforward to produce. The electrostatic interactions between the nanoparticles and polymer matrices are also formed when the conducting PPy is embedded with nanoparticle (NP) cores[10].

EMI interference might either reduce the efficiency of sensitive electronic products or prevent them from running properly, and continuous exposure to this radiation is harmful to human health. Because of these problems, research has centered on creating shielding materials that either take in or block electromagnetic radiation[11]. Certain materials, including metals and various carbonaceous substances (carbon nanotubes, graphene, carbon nanofibers, graphite powder, intrinsically conducting polymers, magnetic and dielectric materials are widely used as promising candidates for shielding industries [12.]

Metal-based materials have been used for a long period to limit EMI, but their heavy weight and corrosion problems make them unfit for use in shielding[13]. Nowadays, technological development has created a need for materials that resist corrosion, are strong, and light in weight. This is the reason why shielding materials such as electrically conducting materials, grounded on conducting polymers and polymer composites, are often used instead of metallic EMI shielding materials due to their lightweight, processability, electrical conductivity, and resilience to corrosion[14]. Composite materials containing conductive fillers are beneficial when protecting systems from EMI. These composites can deliver several important rewards. Better defence against electronic radiation: Conductive fillers can greatly increase the EMI shielding capabilities of a material.

Frequently, polymer composites for EMI shielding are much lighter than conventional shield-metal materials, which may be very helpful when you want to reduce weight.. Flexibility: Since polymer composites are more flexible than traditional EMI shielding materials, they are simpler to fit onto different shapes and surfaces [15]. Conductive C.B is a tiny and inexpensive particle that can make any composite electrically conductive. Adjacent particles interacting tend to lead these particles to group in bigger chains and clusters under the effect of van der Waals forces and electrostatic forces. Consequently, because of its ability to join, it readily produces conductive

structures in rubber or other polymer materials and greatly improves the overall qualities of the composites [16].

Examined the EMI shielding feature of polypyrrole nanostructure and managed to reach −13.5 dB shielding effectiveness in C-band region[17]. Synthesized polypyrrole nanotube composites mixed with nanofibrillated cellulose were analyzed for their electrical and capacitive features and resulted in 75% effectiveness as shielding materials in C-band region[18].

The presented fundamental study focuses on the shielding efficiency of morphologies of PPy /(carbon black) at various concentrations (1, 3 and 5 % w/w) in a composite, and the EMI measurement was made in the C-band , X-band region covering frequencies from 5.85–8.2 GHz, 8.2-12.4 GHz. These regions are especially important for the future application of conducting polymers in the radar, wireless and satellite EMI shielding.

2. Materials and Methods

2.1. Materials

Chemicals Pyrrole (PROSYNTH, 98%, no 63044, Mol.Gew 67.09), The iron(III) chloride hexahydrate powder from Sigma-Aldrich (purity 99%, CAS number 10025-77-1), Methyl Orange powder from Sigma-Aldrich (purity 87%, CAS number 547-58-0), Sunset Yellow FCF powder from Sigma-Aldrich (purity 90%, CAS number 2783-94-0) and sodium hydroxide pellets from Penta (purity 100%, The reactions were all conducted with distilled water as the solvent. A Dow Corning Sylgard 184/catalyst kit was applied as the silicone matrix for transparent C-band PPy studies.

2.2.Preparation of polypyrrole (PPy) and carbon black (PPy/CB) nanocomposites

To produce 1.2 gm of ppy nanofiber initially, it is necessary to achieve thorough and precise dissolving of 0.8 gm of methyl orange (MO) powder into 100 ml of deionized water with 0.05 gm of sodium Dodecyl sulfate (SDS) and 2 ml of pyrrole. The solution is then stirred, and the container is immersed in an ice bath. Following the cooling process, 4.8 gm of ferric chloride into 100 ml of deionized water in ice bath (3–7 °C) to avoid high temperatures, which will significantly assist in controlling the reaction conditions. The solution gradual a change takes place as the solution makes a shift from red to black colour after adding the first solution slowly as drops, therefore signaling the formation of the targeted molecule. In order to ensure the reaction completes without disturbances, it should be done to subjected this combination to magnetic stirring for the entire duration of 24 hours. After a period of time, the precipitate that has been produced is isolated by filtration and then rinsed repeatedly with ethanol and distilled water. The significance of these washing procedures lies in their role in the purification of the end product. The washed precipitate, which has been dried in the oven, is then dried at 60 °C for 30 minutes. This drying process is designed to ensure that the consistency of the final product is not compromised and to prevent any possible material contamination. To produce ppy / CB nano composites, we add the percentage (1,3,5 %) of CB with 60nm (particle size in **Figure 1**) to the solution of methyl orange / SDS/py before oxidation.

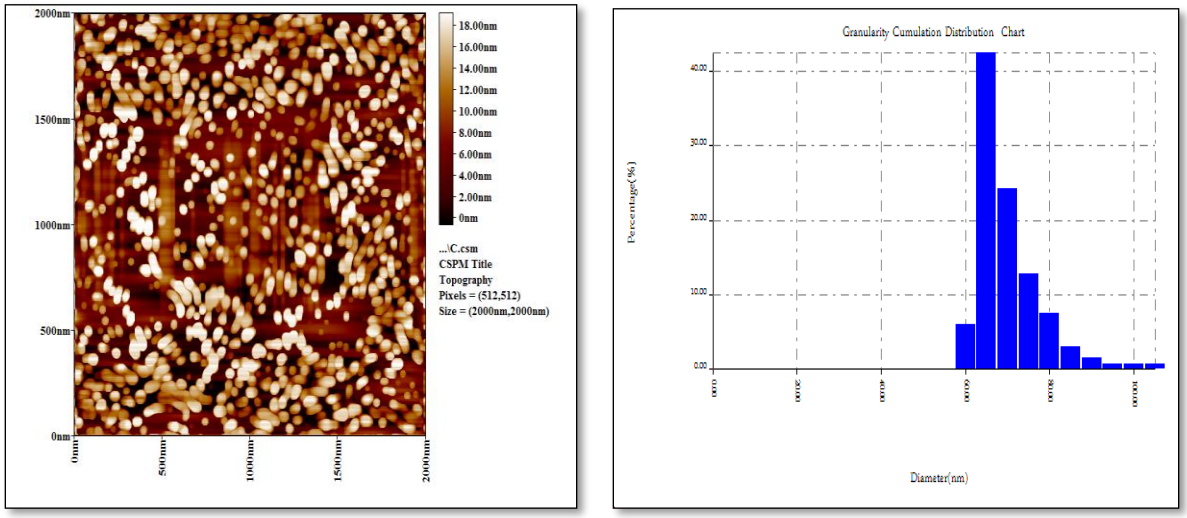

Figure1. Granularity normal distribution chart for carbon black particle

2.3. Characterisation of PPy/carbon black nanocomposites

Fourier Transform Infrared (FT-IR) Analysis type FTIR -7600 was used to record the infrared spectra, which ranged from 400 to 4000 $cm^{-1}.m^{-1}$. XRD patterns were taken from angles between 20 and 80˚ at a step width of 0.02˚ and a step time of 1.25 seconds using CuKα radiation (with a wavelength of 1.5406 Á), FESM offers elemental and topographical information at magnifications ranging from 10x to 300,000x. A.C conductivity σ ac (ω) has been computed with the use of relations

$$\sigma\,\text{total}(\omega) = \sigma\,\text{ac}(\omega) + \sigma\text{dc} \quad \textbf{(1)}$$

$$\sigma\text{ac}(\omega) = \sigma\text{t} - \sigma\text{dc} = \text{A}\omega\ \text{s} \quad \textbf{(2)}$$

In which σ dc represent D.C. conductivity. (A) represent a constant independent on the temperature, (ω =2*π*f) and (s) represents frequency exponent [19 , 20.]

Dielectric permittivity of a material (ε) can be described as a complex quantity with a real part (εr) and imaginary part (εi) and it is given by **Equation 3**

$$\varepsilon = \varepsilon r + \varepsilon i \quad \textbf{(3)}$$

The real and imaginary part values of the dielectric permittivity εr and εi can be estimated from the capacitance value that is measured in the parallel mode (Cp) and loss tangent (tan δ). Cp and tan δ values are measured for the temperature of the room and a range of frequency of 10 kHz–100 MHz. The εr and εi values are estimated based on **Equation 4** and **5**:

$$\acute{\varepsilon} = \text{Cpd}\varepsilon°\text{A} \quad \textbf{(4)}$$

$$\hat{\varepsilon} = \acute{\varepsilon}\text{tan}\eth \qquad \text{where } \delta = 90 - \varphi \quad \textbf{(5)}$$

$$\text{tan}\eth = \hat{\varepsilon}/\acute{\varepsilon} \quad \textbf{(6)}$$

where εo represents free space permittivity, and d and A represent the sample's thickness and cross-section area, respectively. Electromagnetic Interference Shielding Effectiveness. With the use of the waveguide method (closed system), the samples' electromagnetic characteristics are measured at X-band frequency. The about 1.3 cm thick preparation samples are cut to fit in the rectangular waveguide's cross-section (2.29×1.02 cm2). To avoid any EM energy leakage, the sample is placed inside the waveguide (sample holder) so that it completely covers the cross-section. 8.2–12.4 GHz incident and transmission powers are used to calculate the shielding effectiveness. Using a network analyzer and the coaxial line approach, the SE of the composite was measured in the frequency range of 4-8.1 GHz (C-band), 8.2GHz to 12.4GHz (X-band). Using the following **Equation 7**, SE was determined and expressed in decibels (dB): EMI SE (SE_{total}) is represented by the summation of contributions from reflection loss (SE_R), absorption loss (SE_A), and multiple reflections (SE_M)[21]

$$\text{SEtotal} = \text{SEA} + \text{SER} + \text{SEM} \quad \textbf{(7)}$$

The amount of Total SE depends on the difference in impedance between the transmission medium and the material (η0 being the impedance of the medium and η being the impedance of the material). Skin thickness (skin depth δ) corresponds to the point where the field reduces to 1/e from what it once was, and its value depends on frequency (f), permeability (μ), and conductivity (σ)[22]:

$$\delta = 1/\sqrt{(f\pi\mu\sigma)} \quad \textbf{(8)}$$

A thermogravimetric analyzer was used at a temperature range of 100–500°C and a 10°C/minute heating speed to observe the weight loss due to increasing temperature (STA PT-1000 linseis, Germany).

3. Results

3.1. Fourier Transform Infrared (FT-IR)

Figure 2 and **Table 1** show the FTIR spectra of PPy powder, PPy/C.B nanocomposites.

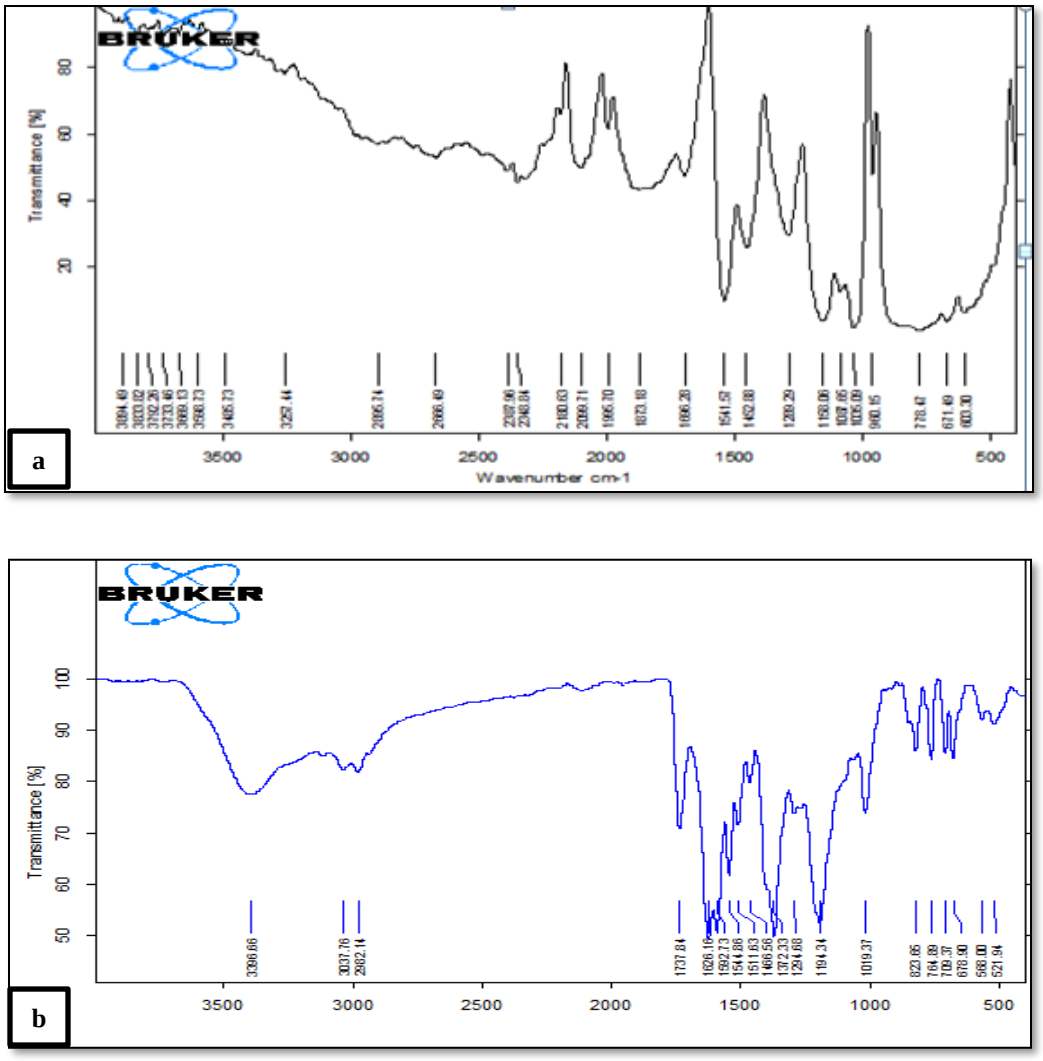

Figure 2. FTIR of (a) PPy and (b)PPy/C.B nanocomposites at 5%

Table 1. FTIR of PPy and PPy/C.B nanocomposites at 5%

No.of bond	Name of bonds
910 cm^{-1}	C–H wagging
1541 cm^{-1} and 1452 cm^{-1}	C=C stretching
1686 cm^{-1} and 1290 cm^{-1}	C=N and C–N bonds
3520 cm^{-1}	N–H stretching vibrations
1146 cm^{-1}	C-H inplane deformation
2887 cm^{-1}	CH aliphatic stretching vibrations
1731 cm^{-1}	C-O stretching mode, of COOH groups
3411 cm^{-1}	OH stretching mode of COOH group
1260 cm^{-1}	C-O stretching mode
1612cm-1	C-C graphitic stretching mode in the carbo
1277 cm^{-1}	C-N stretching vibrations
1594 cm^{-1}	C-C backbone stretching
2890 cm^{-1}	stretching vibration of C-H bond
958 cm^{-1}	C–C out-of-plane ring deformation vibration.
1163cm^{-1}	C–N stretching wagging vibrations

3.2. X-Ray diffraction

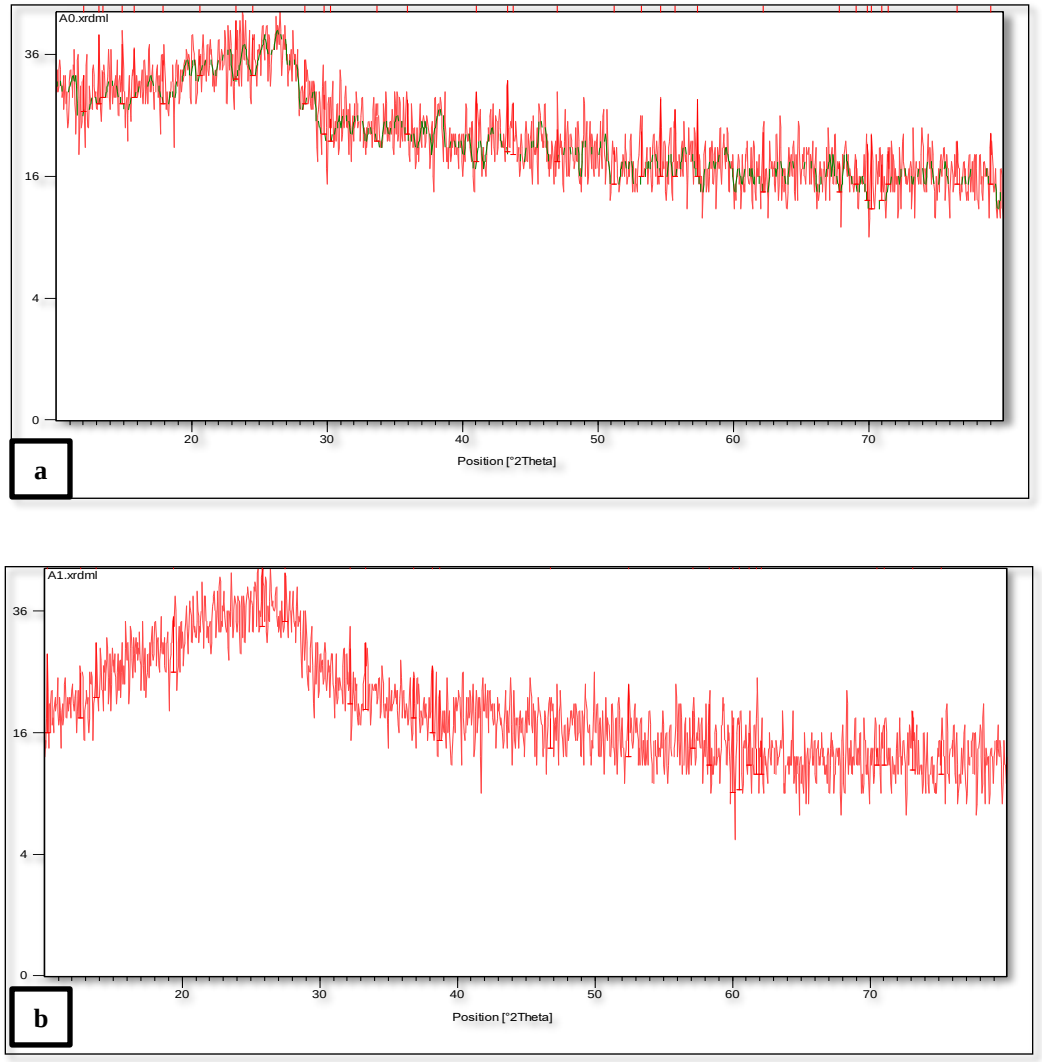

Figure 3.X-Ray of (a) PPy and (b) PPy/C.B nanocomposites at 5%

3.3. Scanning electron microscopy (SEM)

In the **Figure 4** shows the FE-SEM image of PPy.

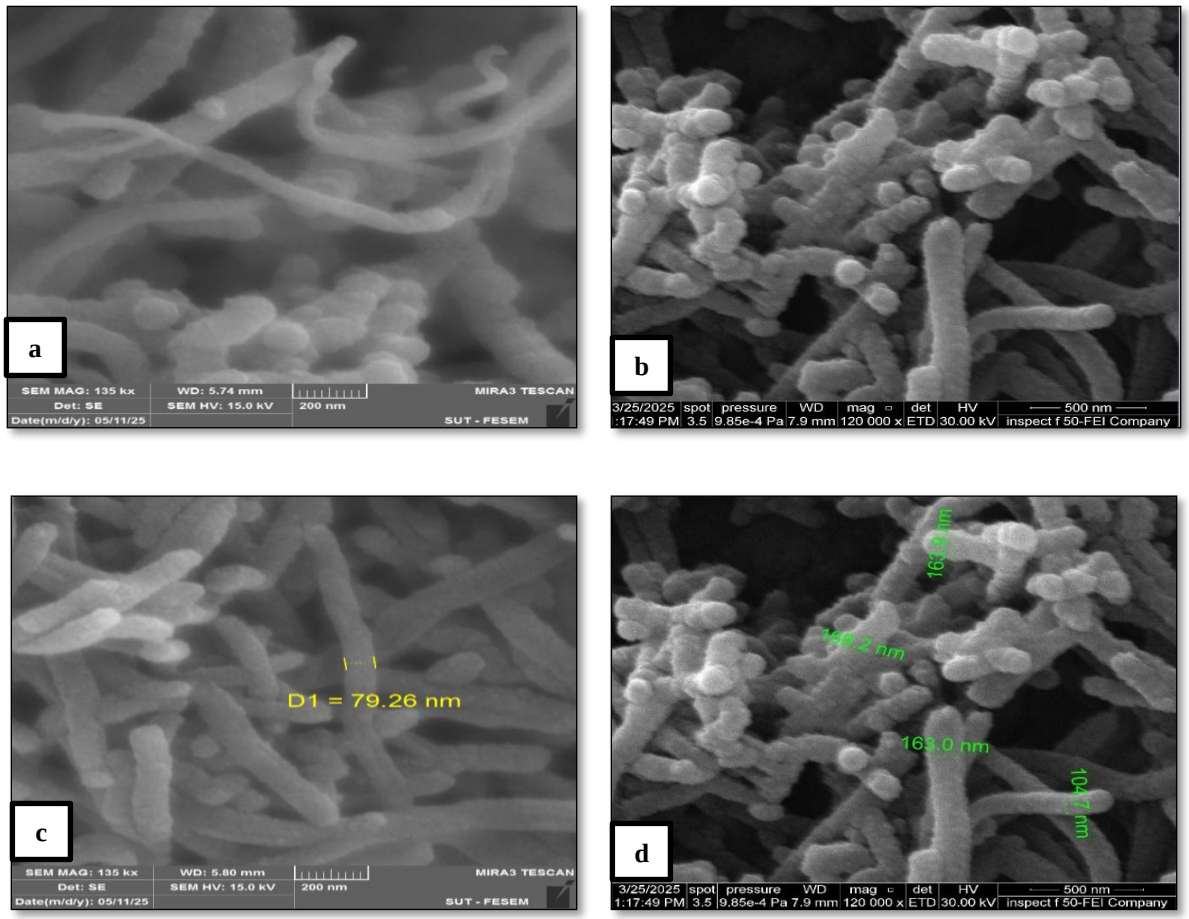

Figure 4. FESM of (a,b) PPy and (c,d) PPy/C.B nanocomposites at 5%

3.4. A.C conductivity

In the **Figure 5** shows the A.C. of PPy at frequencies between $(10^2 - 10^6)$Hz at23°C along with different concentrations of carbon black included.

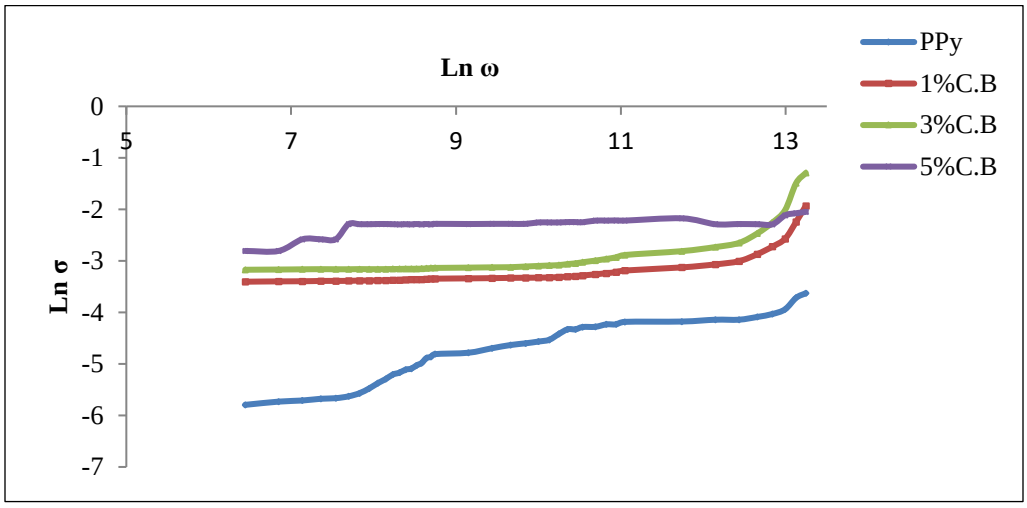

Figure 5. ln(σt(ω)) & Lnω for PPy, PPy/C.B nanocomposites

Table 2: The exponential factor of PPy, PPy/C.B nanocomposites

Samples	S
PPy	0.31
PPy/1%C.B	0.17
PPy/3%C.B	0.13
PPy/5%C.B	0.055

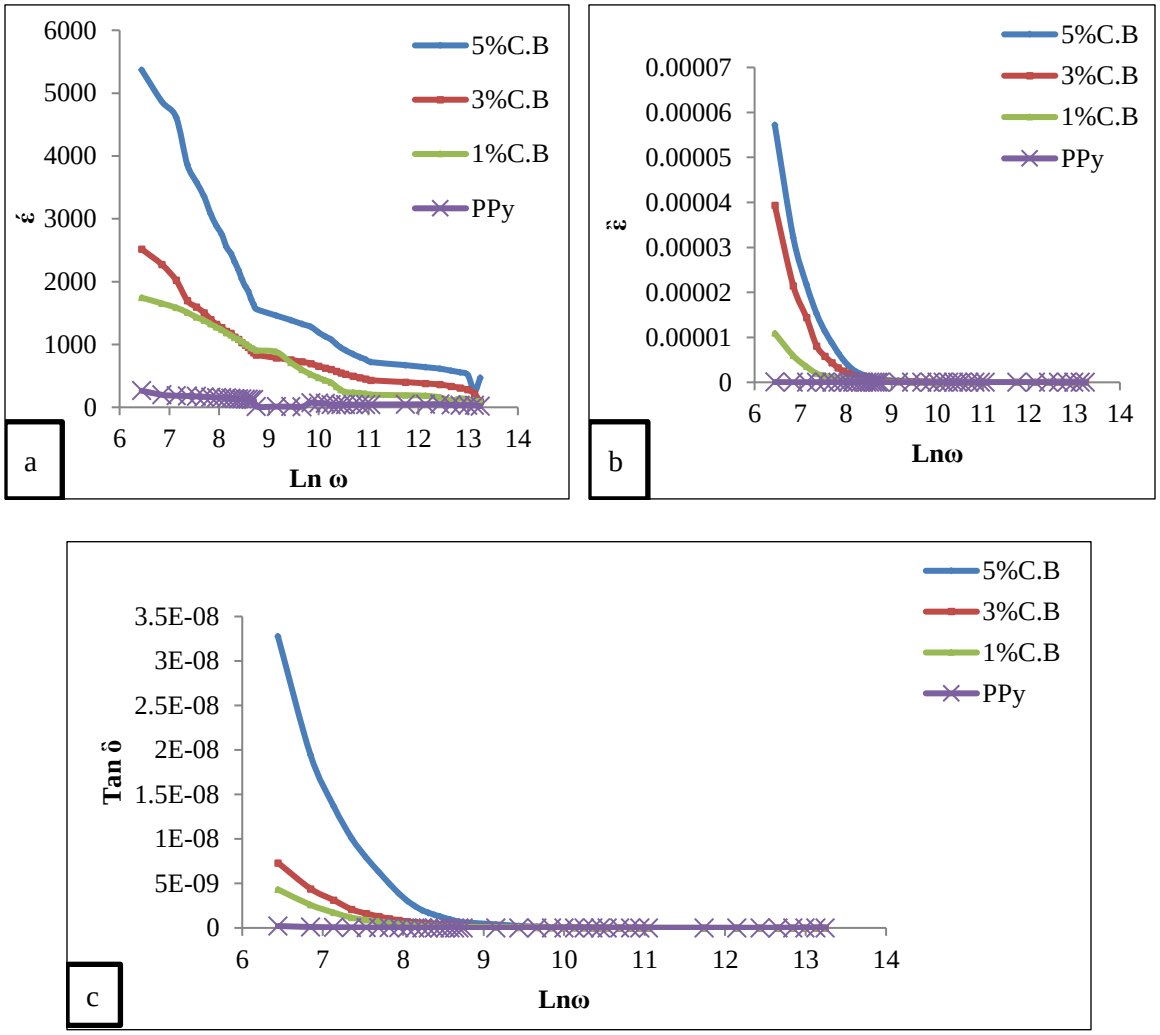

Figure 6. (a) Dielectric constant ε′, (b) Dielectric Loss ε′′, (c) loss tangent tan δ versus Lnω for ppy/C.B nanocomposites at the temperature of 323 K.

3.5 EMI shielding effectiveness

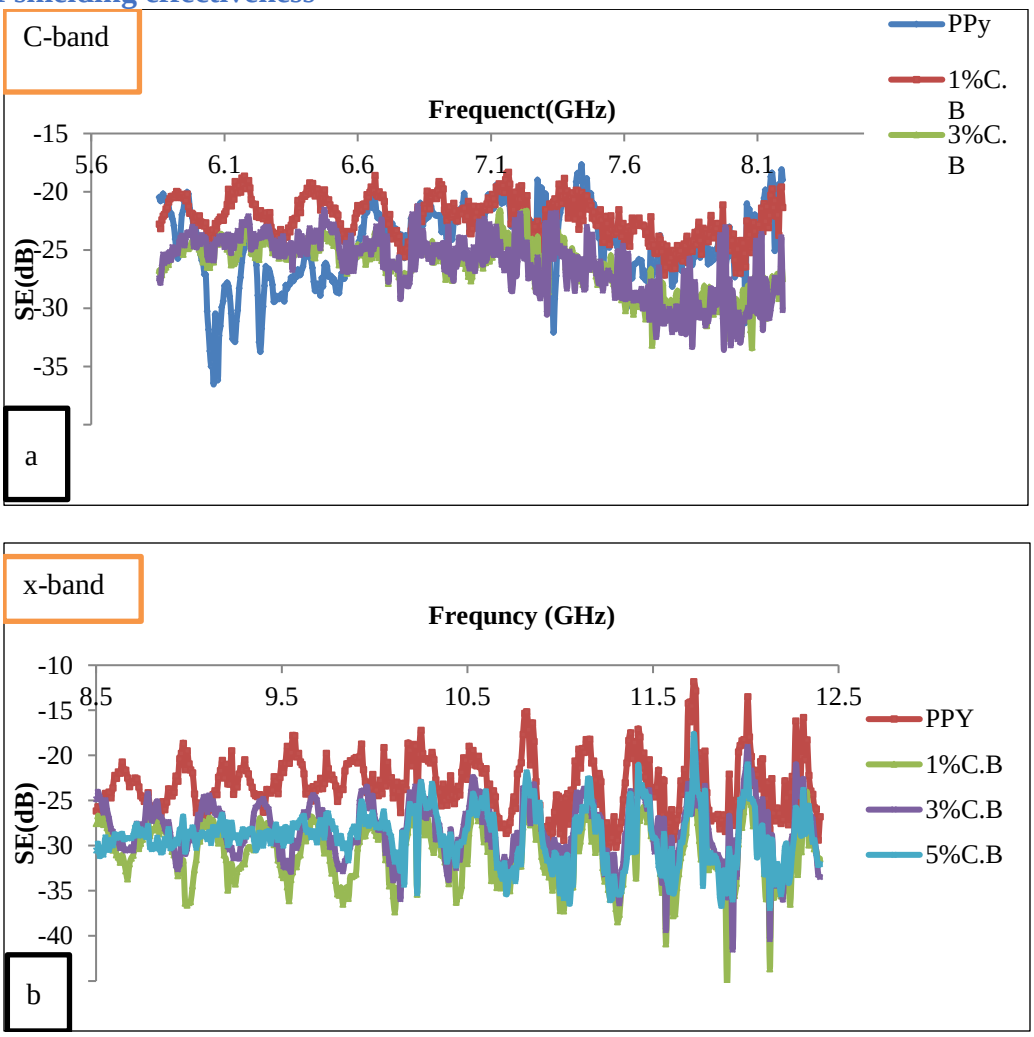

Figure 7. EMI shielding effectiveness of (a) (C-band), (b) (X-band)

3.6. TGA-DSC Analysis

Table 3. Values of the parameters (Tg, Tm, Tc, Td) for the PPY/C.B nanocomposites

sample	Tg °C	Tm °C	Tc °C	Td °C
ppy	110			
1%c.b	150	284.30	402.25	663.99
3%c.b	160	285.55	403.50	690.42
5%c.b	160	286.7	401.02	669.51

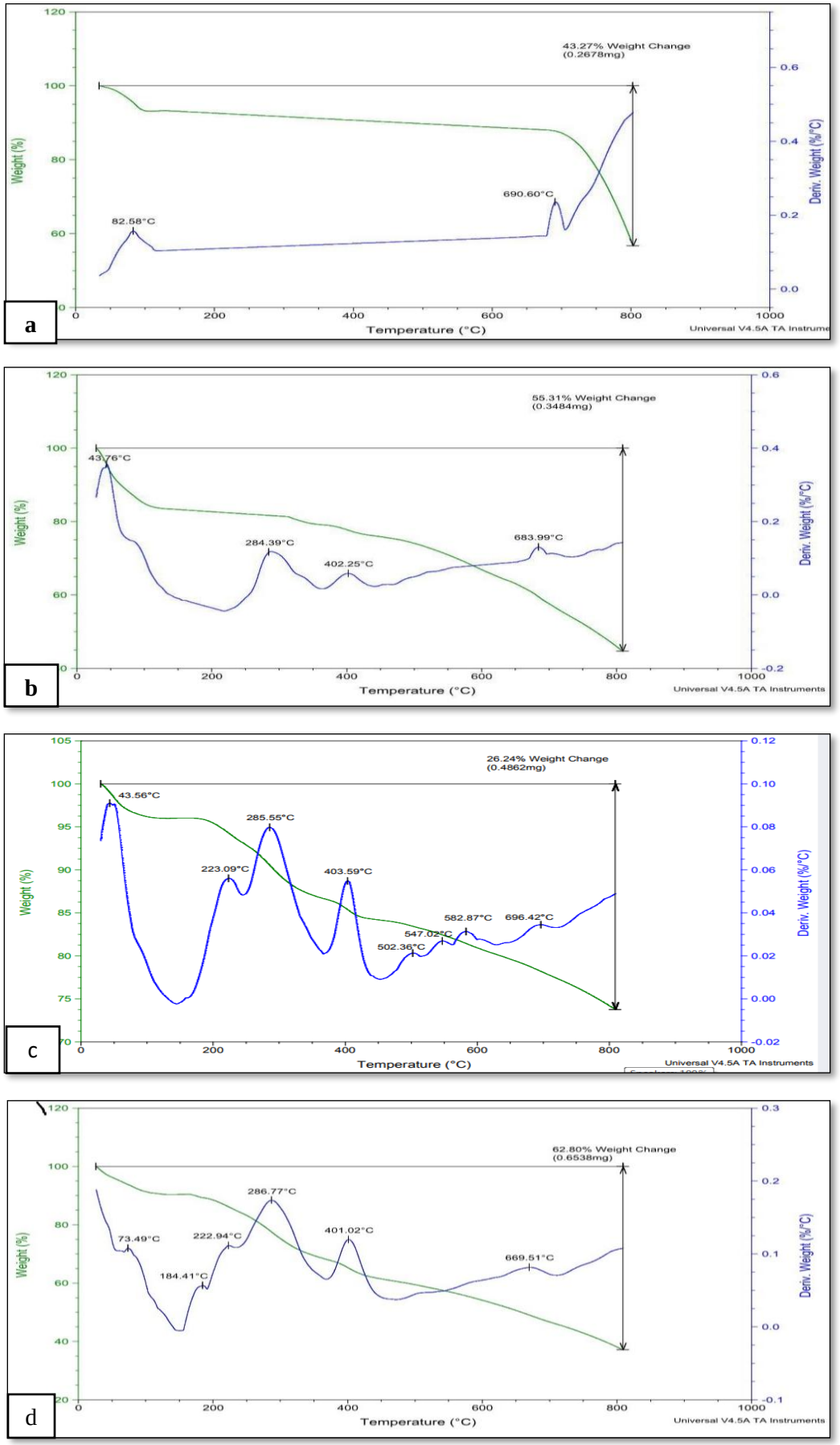

Figure 8. TGA-DSC of (A) PPy and (B)PPy/C.B nanocomposites at 1%, (C)/C.B nanocomposites at 3%, (D)PPy/C.B nanocomposites at 5%

4. Discussion

4.1. Fourier Transform Infrared (FT-IR)

In the **Table 1** and **Figure 2** show the FTIR spectra of PPy powder, PPy/C.B nanocomposites. The peaks at 910 cm^{-1} are attributed to C–H wagging. The characteristic peaks at 1541 cm^{-1} and 1452 cm^{-1} The appearance of a strong peak at 2874 cm^{-1} indicates C=C stretching. Peaks seen at 1686 cm^{-1} and 1290 cm^{-1} indicate C=N and C–N bonds, respectively. Remaining peaks at 3520 cm^{-1} represent the appearance of N–H groups. PPy/carbon black nanocomposites at 5% produced three main peaks on the FTIR readout. The data was recorded at 1277, 1594, 2892, cm^{-1}. C-N stretching was responsible for the peak at 1277 cm-1 and the peak at 1594 cm-1 was due to the vibration of the C-C backbone. The result at 2890 cm-1 comes from stretching vibration of C-H bond agree with[23] and [24]. The peak at 969 nm in absorbance is linked to carbonyl C–O stretching activity, the peak around 701-688 nm to the stretching of the C=C bond in the ring, the peak at 1610 nm shows C=C bending activity and the peak at 2879 nm is due to C≡C stretching in the carbon skeleton of the compounds.

4.2.X-Ray diffraction

In the **Figure 3** reveals that PPy samples are amorphous because their XRD patterns show broad peaks at 2θ = 27˚ originating from PPy chains at the interlunar spacing agree with [24] .The (cs) size from a sharp peak PPy is estimated by using the **Equation 9** Scherrer's formula [25, 26].

$$DK = \lambda/ß\cos\theta \quad \textbf{(9)}$$

Where D is the size of crystallite regions, K is the shape factor equal to 0.89 if we don't know the shape) and θ is the Bragg angle of the most intense peak in the diffraction pattern, and beta is the FWHM in radians equall to 0.1968°. By applying **Equation 11** to the sharp peaks, the mean particle size found in the PPy results is around 62 nm. The diffraction patterns of PPy/C.B nanocomposites were found to be in between those of PPy and carbon. For carbon, the peaks were located at 2θ= 24.5° and 43° correspond to the (002) and (101) lines of the carbon structure, respectively agree with JCPDS Card Files, No. 41-1487 for carbon bkack.

4.3. EF-SEM

In the **Figure 4** shows the FE-SEM image of PPy which has a relatively uniform shape and for PPy/carbon black (with 5 wt % of in PPy) composite a very high magnification of SEM images demonstrates that the polymer in the composite forms clusters with two hemispheres. Carbon black particles are formed by polypyrrole's spherical structure into multi particle aggregates and distributed equally. The results indicate that ultrasonication has eliminated any clustering of PPy particles. The micrographs show filler particles dispersed more or less homogeneously within the polymer matrix.

4.4. A.C. Conductivity

In the **Figure 5** shows the A.C. of PPy at frequencies between (10^2 -10^6)Hz at23°C along with different concentrations of carbon black included. Adding PPy to carbon black raises its abilities to conduct electricity. Yet, a high concentration of carbon black can make the composite behave mainly according to carbon black's conductivity. The incorporation of PPy/carbon black forms a highly conductive internal structure that improves the material's electrical conductivity, space charge and interfacial polarization. Therefore, the efficiency of storing and using electrical energy in the material is raised [27, 28]. The connectivity and electron transport mechanism of C.B network in the polymeric matrix is revealed by the nanocomposites AC .It has been found that all samples conductivities rise with increasing frequency, also PPy conductivity is high . This could be explained by dipoles' propensity to align themselves with the applied field in polymeric samples . In order to obtain the value of s, a linear fitting between lnσ and lnω was performed using the following relation by [29].

$$Ln\sigma = LnA + Sln(\omega) \quad \textbf{(10)}$$

The plot of conductivity versus frequency in **Figure 5** shows PPy, PPy/C.B nanocomposites at various ratios. The dominance of A.C. conductivity, in which the polarization is slightly altered, is the cause of σac (ω) which is clearly frequency dependent for both pure PPy and for (1% C.B),

i.e., the conductivity is pure A.C., and this is due to the electronic polarization. The ability of composites to conduct electricity improved when they were polymerized at 5°C, and the polymer chains were better connected, allowing electron movement to be easier. The plot of ln(σt(ω)) & ln(ω) for PPy /C.B nanocomposites at various ratios provided the (s). For all samples of composites, values of s are quite lawful, as shown in **Table 2**. The exponential factor (s) is smaller than one shows that conductivity occurs during hopping, which reflects the percentage of reactants that have approached and crossed the activation energy hill in the number of tries. The average values of (s) seem to agree with charge carriers (protons) hopping across polymer chains[30]. All of the PMMA/Gr/Ag nanocomposites have had their dielectric **Figure 6** shows the dielectric loss, dielectric constant, Tanὃ with frequency for all composites; at higher frequencies, the loss becomes nearly constant at lower concentrations of graphene, while at greater concentrations of carbon black that mean the dielectric behavior of all fabricated samples was dependence on the carbon black content within the PPy was analyzed.At lower frequency, the carbon black content in the composite determines the dielectric behaviorThe behavior repeats itself for other frequencies down to 1 MHz and the dielectric constant increases linearly with more graphene content, dividing by two at 5% C.B. Because of the presence of carbon black, the conducting chains of PPy became linked, making it easier for the charges to travel between the chains and respond to the electric fields found in microwave radiation. More charge transport across longer ranges and a larger number of relaxation paths caused an increase in the amount of absorbed energy. Additionally, SE was improved by higher microwave absorption, thanks to the increased space charge and stronger polarization caused by the difference in dielectric constants between carbon black and the PPy polymer. The dielectric constant (ε′) and the dielectric loss (ε″) got marginally smaller when carbon black is present in higher concentrations in the Ppy matrix, suggesting the percolation effect.

4.5. EMI shielding effectiveness

The investigation is performed in the C-band region within the 5.37–8.2 GHz microwave frequency range. This range is particularly relevant for PPy's potential application in EMI shielding due to its use in various communication technologies like radar, wireless communication, and satellite communication.. Resulting in a remarkable EMI SE of (-20 to –36) dB at 1, 3, 5% loading of carbon black. The analysis of composite materials using x-band EMI-SE was carried out on samples containing various levels of PPy/C.B in the Frequency range of(8.2 to 12.4) GHz. The behaviour of the C.B filler in combination with the polymeric matrices was studied. The total SE displayed in **Figure 7** improved as the electrical conductivity of the composites becomes higher. EMI shielding efficiency since they are capable of reaching higher electromagnetic shielding values with lower amount of CB in -PPy between (-10 to -45.6)dB. The effectiveness of a uniform PPy shielding layers in the C-band region is mainly determined by its electrical conductivity. Furthermore, Most applications of electromagnetic shielding materials need to achieve at least a −20 dB reduction in electromagnetic waves, which corresponds to the shielding of more than 99% of the incident radiation. Even though reflection causes secondary pollution, carbon-based composites are usually able to achieve high EMI shielding through their electrical properties[22,25, 31.] The link between EMI shielding and carbon black concentration depends on the two mechanisms – Ohmic loss and polarization loss. As shown in **Figure 8.** A single conductive filler is viewed as a kind of resistor for moving charges and a pair of conductive fillers with a polymer binding them can be seen as a capacitor with nanometer-scale features. Consequently, it can be argued that a CPC has a large number of resistors and capacitor structures arranged in series or parallel form. An increased quantity of both carbon black and composite materials is being used. Thickness leads to a greater number of both resistor and capacitor structures, resulting in higher Ohmic loss and polarization loss, respectively. Actually, the more conductive filler is used, the more nematic, electric and magnetic dipoles can interact with localized charges. This helps the EM wave get weakened much more smoothly. EMI-SE is a relationship involving electrical conductivity [23] .

$$SE = 50 + 10\text{Log}\left(\frac{\sigma}{f}\right) 1.7t\sqrt{\sigma f} \quad \textbf{(11)}$$

where σ (S m^{-1}), t (cm) and f (MHz) are the electric conductivity, thickness and frequency of the shielded materials, respectively. For EMI shielding materials, an EMI SE greater than 20 dB means that 99% of electromagnetic waves can be blocked and these materials comply with the commercial requirements.

4.6. TGA-DSC Analysis

In the **Figure 9, Table 3** illustrates how much weight loss occurs for PPy and PPy C.B nanocomposites in nitrogen at temperatures ranging from 25 to 800 °C as the heating rate is 10 °C $minute^{-1}$. PPY samples followed three stages in the TGA curve during weight loss. In a thermogram of pure polypyrrole, the weight loss is recorded from about 40°C all the way up to 150°C. and the other is at 150-650°C and then a rapid mass loss occurred from 650 °C to 800 °C. First, the main loss occurs when water molecules are removed because of the sample's moisture and solvent. After that, the loss increases when oligomers leave the sample. The main reason for a significant weight reduction at temperatures over 150 °C in samples is the decomposition of PPy. The carbon black did not change much and mostly remained stable when heated from 25 to 800°C. Studies showed that PPy decomposed at temperatures between 25 and 800°C, whereas carbon black was still intact up to 800°C.

In pure PPy, DSC reveals a wide endotherm at approximately 110 °C which denotes the glass-transition temperature (Tg) of PPy. The Tg of PPy in the nanocomposites is influenced by the presence of carbon black nanoparticles. Also, there is a peak found at 295.2 °C in PPy which signals the PPy melting point. Nonetheless, the presence of nanoparticles changes how the meting temperature of PPy will behave in these polymer nanocomposites. Initial reports indicate that nanocomposites are promising in nanohybrid materials. show a high melting temperature at 284, 285.9, and 287.3 °C, respectively. PPy has a greater melting point in nanocomposites with a larger amount of carbon black which is explained by the high level of crystallinity in PPy seen through XRD.

5. Conclusion

Images from FE-SEM reveal details about the appearance and structure of the PPy/carbon black nanocomposite. which can be modified to improve the organization of the components, giving the material better conductivity and shielding qualities. One reason carbon-based fillers are preferred is that their unique qualities rely mainly on their structure. Consequently, only small amounts of carbon fillers are necessary to benefit the transport characteristics of polymer nanocomposites. The effectiveness of EMI shielding for a material relies largely on its aspect ratio, size, dielectric constant, magnetic properties, interior filler conductivity, and its physical form. The MEI-SE of the nanocomposites resulted in being directly related to their A.C, i.e., the presence of the C.B in the synthesis of PPy. In fact, when the specimens are more conductive, they reported better electromagnetic shielding, since more particles that can interact with the radiation are present, which is useful for particular technological tasks. Ppy composites with carbon black (5%) have greater microwave absorption than other forms of Ppy. Based on the results, the X-band and C-band shielding characteristics and useful dielectric properties of these composites clearly support their use for shielding within these frequency ranges. With the addition of nanocarbon fillers, the introduction of nanofillers alters the degree of crystallinity (Tc) and glass transition temperature (Tg) , due to their enhanced conducting of the polymer matrix have opened a new perspective in the field of EMI shielding.

Acknowledgments

The Department of Physics at Baghdad University's College of Science supported this study.

Conflict of Interest

The authors declare that they have no conflicts of interest.

Funding

None.

References

1. Akram S, Ashraf M, Javid A, Abid A, Ahmad S, Nawab Y, Shaker K. Recent advances in electromagnetic interference (EMI) shielding textiles: A comprehensive review. Synth Met. 2023;294:117305. https://doi.org/10.1016/j.synthmet.2023.117305
2. Ghosh S, Remanan S, Mondal S, Ganguly S, Das P, Singha N, Das NC. Mechanically robust full IPN strengthened conductive cotton fabric for high strain tolerant EMI shielding. Chem Eng J. 2018;344:138–154. https://doi.org/10.1016/j.cej.2018.03.093
3. Zhu L, Zeng X, Chen M, Yu R. Controllable permittivity in 3D Fe_3O_4/CNTs network for remarkable microwave absorption. RSC Adv. 2017;7:26801–26808. https://doi.org/10.1039/C7RA04456A
4. Wanasinghe D, Aslani F. Recent advancements in EMI shielding metallic materials and processes: A review. Compos Part B Eng. 2019;176:107207. https://doi.org/10.1016/j.compositesb.2019.107207
5. Wu Y, Zhao Y, Zhou M, Tan S, Peymanfar R, Wang J, Liu P, Li X. Ultrabroad microwave absorption and infrared stealth of CuS@rGO aerogels. Nano Micro Lett. 2022;14:171. https://doi.org/10.1007/s40820-022-00906-5
6. Al-Saleh MH. Electrical, EMI shielding and tensile properties of PP/PE blends filled with GNP/CNT. Synth Met. 2016;217:322–330. https://doi.org/10.1016/j.synthmet.2016.04.023
7. Al-Saleh MH, Saadeh WH, Sundararaj U. EMI shielding effectiveness of carbon-based nanostructured polymers. Carbon. 2013;60:146–156. https://doi.org/10.1016/j.carbon.2013.04.008
8. Mondal S, Das P, Ganguly S, Ravindren R, Remanan S, Bhawal P, Das NC. Thermal-air ageing effects on CNT polymer nanocomposites. Compos Part A Appl Sci Manuf. 2018;107:447–460. https://doi.org/10.1016/j.compositesa.2018.01.025
9. Jeddi J, Katbab AA. Electrical conductivity and EMI shielding of PU/SR/CB/nanographite composites. Polym Compos. 2017;39:3452–3460. https://doi.org/10.1002/pc.24363
10. Pan Y, Liu X, Hao X, Starý Z, Schubert DW. Enhancing conductivity of carbon black-filled immiscible polymer blends. Eur Polym J. 2016;78:106–115. https://doi.org/10.1016/j.eurpolymj.2016.03.019
11. Kumar GS, Patro TU. Electromagnetic interference shielding and radar absorbing properties of carbon nanotube polymer films. Mater Res Express. 2018;5:115304. https://doi.org/10.1088/2053-1591/aade39
12. Kuester S, Barra GMO, Demarquette NR. Morphology and electromagnetic interference shielding of SEBS/CNT nanocomposites. Polym Int. 2018;67:1229–1240. https://doi.org/10.1002/pi.5630
13. Sharma SK, Gupta V, Tandon RP, Sachdev VK. Synergic effect of graphene and MWCNT on electromagnetic interference shielding. RSC Adv. 2016;6:18257–18265. https://doi.org/10.1039/C5RA23418B
14. Chen Z, Xu C, Ma C, Ren W, Cheng HM. Lightweight and flexible graphene foam composites for high-performance electromagnetic interference shielding. Adv Mater. 2013;25:1296–1300. https://doi.org/10.1002/adma.201204196
15. Szeluga U, Kumanek B, Trzebicka B. Synergy in hybrid polymer/nanocarbon composites: A review. Compos Part A Appl Sci Manuf. 2015;73:204–231. https://doi.org/10.1016/j.compositesa.2015.02.021
16. Wu J, Ye Z, Ge H, Chen J, Liu W, Liu Z. Carbon fiber/magnetic graphene/epoxy composites with enhanced electromagnetic interference shielding effectiveness. J Colloid Interface Sci. 2017;506:217–226. https://doi.org/10.1016/j.jcis.2017.07.020
17. Rani P, Malik RS. Electromagnetic interference shielding behavior of polypyrrole-impregnated PEI/SPEEK composites. Mater Chem Phys. 2023;307:128187. https://doi.org/10.1016/j.matchemphys.2023.128187
18. Lapka T, Kopecký D, Mazúr P, Prokeš J, Ulbrich P, Dendisová M, Stejskal J. Nanofibrillated cellulose composites with polypyrrole nanotubes for flexible electronics. Synth Met. 2021;278:116806. https://doi.org/10.1016/j.synthmet.2021.116806

19. Alawi BI, Ali NA. Enhanced electromagnetic interference shielding performance of PMMA/graphene/silver hybrid composites. Ibn Al-Haitham J. Pure Appl. Sci. 2024;37(4): 207–225. https://doi.org/10.30526/37.4.3604.
20. Jawad MK, Noori FTM, Hussein SI, Ali NA, Muslim ZR, Saleh MA. Polypyrrole-functionalized multiwalled carbon nanotube heterojunctions for gas detection applications. Iraqi J Appl Phys. 2024;20(3):573–576.
21. Wei LS, Mao SC, Ming ML, Song B, Chan YW, Jia L, Lau SP. Flexible graphene/polymer multilayered sandwich films for high-performance electromagnetic interference shielding. Carbon. 2014;66:67–76.
22. Farzaneh F, Pei LY, Ramesh UK, Gedler G, Antunes M, Velasco JI, Covas JA. Enhanced electromagnetic interference shielding effectiveness of polycarbonate/graphene nanocomposites via supercritical CO_2 processing. Mater Des. 2016;90:906–914. https://doi.org/10.1016/j.matdes.2015.11.040
23. Nehru R, Gnanakrishnan S, Senthil Kumar B, Chen CE, Dong CD. Polypyrrole–carbon black/$BiPO_4$ composites for sensing and environmental applications. Process Saf Environ Prot. 2024;184:790–803. https://doi.org/10.1016/j.psep.2024.01.023
24. Ahmed FM, Hassan SM, Kamil MI. DC electrical conductivity of polypyrrole/graphene nanocomposites. Iraqi J Phys. 2020;18(44):50–61.
25. Hussein SI, Hashim AA, Jasim SM, Ali NA, Ali IH, Rashad M, Ahmed FM. Acrylic/graphene hybrid polymers with enhanced electromagnetic interference shielding properties. Diam Relat Mater. 2025;154:112190. https://doi.org/10.1016/j.diamond.2025.112190
26. Memioglu F, Bayrakceken A, Oznuluer T, Ak M. Polypyrrole/carbon composite materials as catalyst supports for hydrogen energy applications. Int J Hydrogen Energy. 2012;37(21):16673–16679. https://doi.org/10.1016/j.ijhydene.2012.08.095
27. An H, Wang Y, Wang X, Zheng L, Wang X, Yi L, Feng J. Polypyrrole/carbon aerogel composites for high-performance supercapacitor electrodes. J Power Sources. 2010;195(19):6964–6969. https://doi.org/10.1016/j.jpowsour.2010.05.008
28. Ansari R. Polypyrrole conducting electroactive polymers: Synthesis, characterization, and stability. E-J Chem. 2006;3(13):186–201. https://doi.org/10.1155/2006/860413
29. Heiba ZK, Ghannam MM, Sanad MMS, Albassam AA, Mohamed MB. Structural, optical, and dielectric properties of nano-$ZnMn_2$−xVxO_4 materials. J Mater Sci Mater Electron. 2020;31:8946–8962. https://doi.org/10.1007/s10854-020-03429-0
30. Gao C, Chen G. Conducting polymer/carbon thermoelectric composites: A review. Compos Sci Technol. 2016;124:52–70. https://doi.org/10.1016/j.compscitech.2016.01.004
31. Wang L, Jiang J, Xu J, Zhou W, Li C, Sun H, Zhang Q. Effects of second dopants on electrical conductivity and morphology of PEDOT:PSS/carbon black composites. Mater Chem Phys. 2015.